

Published in final edited form as:

*Biomacromolecules*. 2011 November 14; 12(11): 4127–4135. doi:10.1021/bm201198x.

## Influence of Injectable Hyaluronic Acid Hydrogel Degradation Behavior on Infarction Induced Ventricular Remodeling

Elena Tous<sup>1</sup>, Jamie L. Ifkovits<sup>2</sup>, Kevin J. Koomalsingh<sup>2</sup>, Takashi Shuto<sup>2</sup>, Toru Soeda<sup>2</sup>, Norihiro Kondo<sup>2</sup>, Joseph H. Gorman III<sup>2</sup>, Robert C. Gorman<sup>2,+</sup>, and Jason A. Burdick<sup>1,\*</sup>

<sup>1</sup>Department of Bioengineering, University of Pennsylvania, Philadelphia, PA, 19104, USA

<sup>2</sup>Gorman Cardiovascular Research Group, University of Pennsylvania, Glenolden, PA, 19036, USA

### Abstract

Increased myocardial wall stress after myocardial infarction (MI) initiates the process of adverse left ventricular (LV) remodeling that is manifest as progressive LV dilatation, loss of global contractile function, and symptomatic heart failure, and recent work has shown that reduction in wall stress through injectable bulking agents attenuates these outcomes. In this study, hyaluronic acid (HA) was functionalized to exhibit controlled and tunable mechanics and degradation once crosslinked, in an attempt to assess the temporal dependency of mechanical stabilization in LV remodeling. Specifically, two hydrolytically degrading (low and high HeMA-HA, degrading in ~3 and 10 weeks, respectively) and two stable (low and high MeHA, little mass loss even after 8 weeks) hydrogels with similar initial mechanics (low: ~7 kPa, high: ~35–40 kPa) were evaluated in an ovine model of MI. Generally, the more stable hydrogels maintained myocardial wall thickness in the apical and basilar regions more efficiently (low MeHA: apical: 6.5mm, basilar: 7mm, high MeHA: apical: 7.0mm basilar: 7.2mm) than the hydrolytically degrading hydrogels (low HeMA-HA: apical: 3.5mm, basilar: 6.0mm, high HeMA-HA: apical: 4.1mm, basilar: 6.1mm); however, all hydrogel groups were improved compared to infarct controls (IC) (apical: 2.2mm, basilar: 4.6mm). Histological analysis at 8 weeks demonstrated that although both degradable hydrogels resulted in increased inflammation, all treatments resulted in increased vessel formation compared to IC. Further evaluation revealed that while high HeMA-HA and high MeHA maintained reduced LV volumes at 2 weeks, high MeHA was more effective at 8 weeks, implying that longer wall stabilization is needed for volume maintenance. All hydrogel groups resulted in better cardiac output (CO) values than IC.

### Keywords

Hyaluronic Acid; Hydrogel; Cardiac Remodeling; Degradation; Mechanical Properties

### Introduction

Recently, left ventricular (LV) remodeling caused by myocardial infarction (MI) has been implicated in approximately two-thirds of the 5 million annual cases of heart failure<sup>1</sup>. MI results from the occlusion of a coronary artery, leading to the depletion of oxygen and nutrients and resulting in cardiomyocyte necrosis and extracellular matrix (ECM) breakdown. As the ECM is disrupted, the myocardium is susceptible to expansion and

\*burdick2@seas.upenn.edu. Tel: 215-898-8537. Fax: 215-573-2071. +Robert.Gorman@uphs.upenn.edu. Tel: 267-350-961. Fax: 267-350-9627.

dilation, leading to geometric changes that subsequently increase stress throughout the injured and healthy regions of the heart<sup>2-5</sup>. These maladaptive responses lead to a series of biological changes that cause further cell death and increase myocardial instability, which contribute to contractile dysfunction and can progress into a positive feedback loop that ultimately leads to heart failure<sup>6-9</sup>. The strategy in this investigation was to target initial infarct expansion (stretching), which has been identified as the initiator of the maladaptive events associated with adverse post-MI remodeling<sup>10-12</sup>.

Theoretical<sup>3, 13, 14</sup> and experimental models<sup>15-33</sup> have shown that limiting infarct expansion with the introduction of injectable materials into the infarct can attenuate the remodeling process, primarily through bulking (thickening) and stabilizing (stiffening) the infarct zone. Specifically, finite element (FE)<sup>13, 14</sup> models have demonstrated that injecting bulking materials into the infarcted myocardium decreases fiber stress, the extent being dependent on material stiffness<sup>13</sup>, volume<sup>13, 14</sup>, and distribution<sup>14</sup>. Experimental models have tested a variety of both natural<sup>15-28</sup> and synthetic<sup>30-33</sup> materials as injectable agents and demonstrated varying degrees of success. The materials tested to date have had a wide range of properties, including the method of gelation, bulk mechanical properties and degradation behavior. Few studies have been performed to determine the optimal mechanical and degradation properties for the injected material; although, based on theoretical analyses both parameters should affect efficacy.

Tunable hydrogel systems provide an important experimental tool to help identify the optimal material properties of the injectate, since material properties (gelation, stiffness and degradation) can be independently manipulated and examined. Ifkovits et al. recently used a mechanically tunable bulking agent to target LV dilation post-MI<sup>18</sup>. Two variations of methacrylated hyaluronic acid (MeHA) were explored, where crosslinking (i.e., mechanics) was adjusted by varying the amount of methacrylation (low and high), yet gelation behavior and mass loss were similar. HA is a naturally occurring linear polysaccharide of alternating D-glucuronic acid and N-acetyl-D-glucosamine<sup>34</sup> and was used in this study to form injectable hydrogels since it is easily functionalized at both its carboxylic<sup>35</sup> and hydroxyl groups<sup>36, 37</sup>. This work concluded that high MeHA was more effective in attenuating LV remodeling and that mechanics are important to consider for bulking agents and in stabilizing the myocardial wall post-MI. In this case both hydrogels were very stable and still present after 8 weeks in an ovine model.

The work described here further delves into properties for injectable hydrogels with a focus on the timing of the material degradation. Hyaluronic acid (HA) was functionalized with hydroxyethylmethacrylate (HeMA), to obtain a crosslinkable macromer (HeMA-HA) that crosslinks similar to MeHA, yet has additional ester bonds that provide further control over hydrogel degradation. Specifically, we compared the previous work<sup>18</sup> of two versions of MeHA hydrogels (low and high mechanics) with the newly synthesized HeMA-HA hydrogels, where initial mechanics were matched and degradation timing was varied. This system is the first to examine the temporal dependency of mechanical stabilization during the progression of LV remodeling, and provides insight into how long mechanical support must be applied to attenuate the aftermath of MI.

## Materials and Methods

The animals studied in this investigation received care in compliance with the protocols from the University of Pennsylvania that were approved by the Institutional Animal Care and Use Committee in accordance with the guidelines for humane care (National Institutes of Health Publication 85-23, revised 1996).

All materials were purchased from Sigma-Aldrich unless otherwise indicated.

### HeMA-HA synthesis

Variations of HeMA-HA were synthesized by coupling HA-tetrabutylammonium salt (HA-TBA) with HeMA-COOH as shown in Figure 1A. HA-TBA was produced by adding an ion exchange resin Dowex-100 to HA-sodium salt (HA-Na, Lifecore, 66 kDa) and titrating with tetrabutylammonium hydroxide until the desired coupling of TBA to HA was reached (pH 7.02–7.05)<sup>36</sup>, followed by freezing and lyophilization. HeMA-COOH was synthesized by reacting hydroxyethylmethacrylate (HeMA) with succinic anhydride via a ring opening reaction catalyzed by N-methylimidazole (NMI) in dichloroethane (DCE) at 65°C. The product was washed with aqueous hydrochloric acid to remove excess succinic anhydride, washed with DI-H<sub>2</sub>O to remove water-soluble impurities, and DCE was removed by rotovap. The coupling of HA-TBA to HeMA-COOH was performed in DMSO at 45°C by activating the carboxylic acid on HeMA-COOH with dimethylaminopyridine (DMAP) and di-t-butyl dicarbonate (BOC<sub>2</sub>O) and coupling it to HA-TBA. Purification involved an overnight dialysis against DI-H<sub>2</sub>O at 4°C to remove DMSO, precipitation in acetone, and a final 3 day dialysis against DI-H<sub>2</sub>O at 4°C to remove excess impurities. Methacrylation was adjusted by varying the amount of HeMA-COOH and BOC<sub>2</sub>O and all products were assessed with <sup>1</sup>H NMR (Bruker).

### MeHA synthesis

MeHA was synthesized as previously described through reaction of HA with methacrylic anhydride at pH 8.0 for 24 hours followed by dialysis and lyophilization<sup>35</sup>. Methacrylation was altered by varying the amount of methacrylic anhydride and was assessed with <sup>1</sup>H NMR (Bruker).

### Hydrogel formation and characterization

Macromers were crosslinked through a redox radical polymerization with ammonium persulfate (APS) and tetramethylethylenediamine (TEMED) as initiators<sup>38</sup>. Hydrogels were formed between two glass slides within a teflon mold sealed with vacuum grease by mixing two solutions (each containing 4 wt% of the HA macromer and either APS or TEMED). Gelation was assessed by monitoring the storage ( $G'$ ) and loss ( $G''$ ) modulus using an AR2000ex Rheometer (TA Instruments) at 37°C under 1% strain and a frequency of 1 Hz in a cone and plate geometry (1°, 20 mm diameter). Compression testing was performed on samples immediately after gelation (Day 0) or at desired time points throughout degradation with a Dynamic Mechanical Analyzer (DMA) (Q800 TA Instruments) at a strain rate of 10%/min and moduli were calculated at a strain from 10–20%. For degradation assessment, gels were incubated in PBS at 37 °C and samples were collected at various time points and mass loss was quantified using a uronic acid assay<sup>39</sup>.

### Selection of formulations

Initial studies were performed on 4wt% HeMA-HA samples at 5 mM APS/TEMED to assess hydrogel properties and the influence of methacrylation on hydrogel behavior. To compare HeMA-HA efficacy to that of MeHA in attenuating LV remodeling, two HeMA-HA variations (low and high) were selected and normalized to their respective MeHA (low and high) initial mechanics and gel dispersion by adjusting APS and TEMED concentrations (Table 1). Temporal mechanics and gelation were evaluated and compared between the groups.

### In vivo evaluation in ovine MI model

Low and high HeMA-HA (Table 1) formulations were applied to an established reproducible *in vivo* ovine infarct model to assess their efficacy in limiting LV remodeling<sup>29</sup>. Twenty-one adult male Dorset sheep (35–40 kg) (n=6 low HeMA-HA, n=8 high HeMA-HA, n=7 infarct control) were anesthetized, underwent a left thoracotomy to expose the heart, and were monitored for arterial, ventricular, and pulmonary artery pressure and electrocardiogram throughout the surgery. Baseline echocardiographic and hemodynamic data were first obtained and then followed by infarction, induced via ligation of the left anterior descending (LAD) and second diagonal coronary artery to create an infarct that was ~40% of the distance from the apex to the base of the heart.

Thirty minutes post-MI, HeMA-HA treatment sheep received twenty 0.3 mL injections in the infarct area of the pre-polymer solution that was mixed for 2 to 3 minutes, depending on the polymer, before injection and gelation. Hemodynamic data and real-time three-dimensional echocardiographs (3DE) were collected before infarction, 30 minutes post-MI, 30 minutes post injection, and 2 and 8 weeks after therapy. 3DE was used to quantify the extent of global LV remodeling by measuring LV diastolic and systolic volumes at each time point. All volume measurements were normalized to preinfarction values<sup>18</sup>. Functional outcomes were analyzed by evaluating cardiac output (CO), and ejection fraction (EF). Each was evaluated by comparing baseline values to outcomes at 2 and 8 weeks post-MI. Animals were sacrificed at 8 weeks, and morphometric and histologic evaluations were performed on the excised hearts. Results were compared to controls consisting of previously published MeHA work (low MeHA (n=5) and high MeHA (n=7))<sup>18</sup> to determine the efficacy of this system in preventing infarct thinning and limiting global LV remodeling.

Due to the potential influences of degradation on biological activity, both vessel formation and inflammation were evaluated in all groups in paraffin embedded sections at the 8 week time point. Vessels were stained with anti- $\alpha$ -smooth muscle actin ( $\alpha$ -SMA, mouse anti-human, Dako, MO851). The apex, middle, and borderzone (BZ) regions of the myocardium were examined (One section per animal for each region). Vessel density was calculated in three fields of view at 20 $\times$  magnification at the apex and borderzone and in nine magnification views in the middle region of each section. Vessels were identified by positive  $\alpha$ -SMA staining and were quantified in three ways: 1) all vessels greater than 10 $\mu$ m, 2) all vessels with visible lumen greater than 10 $\mu$ m, and 3) all thick vessels (vessels with more than one cell layer comprising the lumen) greater than 10 $\mu$ m.

The inflammatory response was investigated by performing immunohistochemical staining with major histocompatibility complex (MHC) class II (mouse anti-sheep, Serotec, MCA901). Staining was evaluated both near the biomaterial and in the surrounding tissue. Briefly, for immunohistochemical staining, paraffin sections were deparaffinized, hydrated and later quenched for endogenous peroxidase activity for 5 minutes in 4% H<sub>2</sub>O<sub>2</sub> in deionized water. After quenching, samples were washed three times in Dako 1 $\times$  wash buffer and primary antibody was applied at appropriate dilutions in Dako diluent ( $\alpha$ -SMA: 1:500, MHC Class II: 1:10) at room temperature for 30 minutes in a humidified chamber. After incubation, three washes in wash buffer were performed and samples were incubated with HRP labeled polymer (Dako, K4000) for 30 min at room temperature in a humidified chamber. After washing three times in wash buffer, sections were incubated in diaminobenzadine substrate (Vector, SK-4100) at room temperature. Samples were then washed in deionized water to stop the reaction, counterstained in hematoxylin stain, dehydrated and cover slipped.

## Statistical analysis

Data is presented as either mean  $\pm$  SD or mean  $\pm$  SEM, as indicated in each figure legend. All changes in data were assessed using a one-way ANOVA with Tukey's post hoc evaluation to account for differences between groups or time points.  $p < 0.05$  was considered statistically significant for all comparisons.

## Results and Discussion

### HeMA-HA synthesis and characterization

We previously synthesized a methacrylated HA (MeHA) and injected two formulations with varying mechanics into infarcted myocardium and observed mechanically-dependent outcomes<sup>18</sup>. Here, we address another property, degradation, through the synthesis of a new HA macromer that contains additional ester bonds between the HA backbone and reactive methacrylate that are susceptible to hydrolysis. Specifically, the TBA salt of HA was successfully reacted with synthesized HeMA succinate (HeMA-COOH) to form reactive HeMA-HA macromers (Figure 1A). HA modification was quantified by <sup>1</sup>H NMR (Figure 1B) and the number of HeMA groups added was tailored by the ratio of HeMA-COOH to the coupling agent BOC<sub>2</sub>O (Figure 1C). Modification of ~10 to 60% of the HA repeat units was possible by changing this ratio. Previous studies using MeHA demonstrated that alterations in the degree of methacrylation varied the hydrogel crosslink density, which correlated with variations in hydrogel bulk mechanics<sup>18</sup>. Thus, variable modification of HeMA-HA can be used to modify resulting gel properties (i.e., mechanics and degradation).

HeMA-HA was reacted into hydrogels using a redox initiation system by mixing solutions of HeMA-HA containing either APS or TEMED (Figure 2A). With this system, kinetic chains form through the reactive methacrylate groups to form a network with bulk properties dependent on the extent of modification and macromer concentration. These hydrogels are susceptible to both enzymatic degradation of the HA and hydrolysis of the side groups, breaking down into primarily the poly(methacrylic acid) kinetic chains and fragments of HA. Initial characterization studies were performed at constant HeMA-HA (4 wt%) and APS and TEMED (5mM APS and TEMED) concentrations to independently evaluate the influence of HeMA modification on material properties. Gelation was examined by performing a time sweep upon mixing of the component solutions, where gel onset was defined as the intersection of the storage ( $G'$ ) and loss ( $G''$ ) modulus (Figure 2B). Unlike MeHA polymers, increases in HeMA-HA methacrylation led to accelerated gel onset times (Figure 2C), potentially due to changes in viscosity with HeMA-HA modification. As expected, increased methacrylation led to increased compressive moduli and times for degradation due to the greater crosslink density and number of bonds needing to hydrolyze for complete hydrogel degradation (Figure 2D).

### HeMA-HA selection

To address how both mechanics and degradation influence adverse LV remodeling, we investigated two variations (low and high) of two different macromers (HeMA-HA and MeHA) (4 hydrogel groups in total), where two hydrogels with low mechanics were compared and two hydrogels with high mechanics were compared, each having variable degradation behavior. Specifically, the HeMA-HA tunability was used to identify two formulations for direct comparison to low and high MeHA from a previous study<sup>18</sup>, where the initial material properties (i.e., initial mechanics and gel dispersion) were similar, but degradation was more rapid than their respective MeHA counterpart due to the addition of hydrolytic degradation in HeMA-HA to the enzymatic degradation mechanism displayed by all HA polymers (i.e., low HeMA-HA vs. low MeHA and high HeMA-HA vs. high MeHA) (Table 1).

As previously mentioned, material properties such as gel dispersion and bulk mechanics can also be influenced by initiator concentrations<sup>18</sup>. As shown in Figure 2, HeMA-HA mechanics and gelation behavior were both dependent on methacrylation; however, MeHA mechanics were influenced by modification, but its gel onset properties were not significantly affected. To compensate for this discrepancy, initiator concentrations were tailored for HeMA-HA formulations (Table 1) to achieve appropriate gelation and mechanical properties that were similar to MeHA hydrogels. While altering the initiator concentration was sufficient to normalize low HeMA-HA gelation to that of MeHA, high HeMA-HA gelation was more accelerated despite initiator adjustments (data now shown). Thus, the gelation time (between injection and reaching gel point) was normalized in the *in vivo* work by injecting high HeMA-HA at 2 minutes, while low HeMA-HA and low and high MeHA were injected at 3 minutes. All gels were analyzed at 4 wt%.

### HeMA-HA and MeHA degradation behavior

HA is enzymatically degradable at its backbone, however, this is dependent on the availability of hyaluronidases and free radicals<sup>35, 36, 40</sup>. Although MeHA does have an ester bond where the methacrylate attaches to HA, accessibility to this bond is sterically hindered and hydrolytic degradation is minimal. Therefore, MeHA degradation is primarily dependent on an enzymatic mechanism and will be referred to as having stable degradation throughout this report. HeMA-HA, however, has additional ester bonds that are accessible for hydrolytic degradation. Thus, in addition to the enzymatic mechanism of the HA backbone, HeMA-HA hydrogels undergo hydrolytic bulk degradation due to the availability of water throughout the gels. As seen in the degradation profiles (Figure 3A), both MeHA formulations lose little mass throughout the 8 week period, yet both HeMA-HA formulations degraded within 8–10 weeks, depending on the extent of modification. Since the HA is reacted via many groups into the kinetic chains, there is minimal mass loss at early time periods even with crosslink hydrolysis, which accelerates at late times when the HA chains can be released from the network, and eventually completely converts to soluble products.

This hydrolysis also leads to exponential decreases in HeMA-HA mechanics, even more rapidly than mass loss, since hydrolysis can cleave the crosslinks and lead to decreases in mechanics prior to releasing mass into the surroundings (Figure 3B)<sup>41–45</sup>. MeHA hydrogel degradation profiles showed an initial minimal burst response that is commonly observed in hydrogels due to a soluble fraction, followed by stable, or minimal, degradation. Slight mechanical decreases in MeHA hydrogels were observed over this period. Overall, it is evident from degradation and mechanical temporal profiles that hydrolytic degradation was more influential in HeMA-HA hydrogels compared to MeHA hydrogels. Importantly, release of HA may also have some biological function. In its linear form, HA plays an active role in wound healing by promoting cell migration and differentiation and angiogenesis, and is involved in heart morphogenesis and development<sup>46–50</sup>. The influence of all treatment groups on local vessel density and inflammation will be discussed in more detail in the *in vivo* portion of this report. Beyond this evaluation, it is not clear how the quantity of HA and its relatively slow release influence the surrounding tissue.

### In vivo evaluation in ovine MI model

As previously discussed, LV remodeling refers to the complex series of events that occur post-MI. Briefly, initial ECM breakdown triggers infarct dilation that propagates throughout the borderzone (BZ) and remote region of the myocardium<sup>2–5</sup>. This results in thinning of the myocardial wall and in global geometric changes, causing the heart to be susceptible to increased stress<sup>6–8, 10, 11</sup>. Although bulking agents are becoming an attractive therapy to stabilize the myocardium and deter geometric changes<sup>15–33</sup>, there is still a lot that remains to

be elucidated towards optimal properties of the injected material. Theoretical models have implied that material properties may also be important to consider in the mechanism<sup>13, 14</sup>, but this was only recently explored experimentally by Ifkovits et al<sup>18</sup>. Towards the importance of degradation, LV remodeling is a time sensitive process that can be broken down into four main periods of necrosis, acute inflammation, fibrosis and remodeling. In humans, necrosis and acute inflammation occur within the first week, followed by fibrosis for approximately three additional weeks and finally by remodeling for approximately four more weeks<sup>2</sup>. Thus, it is of great importance to understand how the material presence during these various periods after infarction plays a role in the progression of LV remodeling, which is performed here with four material formulations.

Thinning of the infarct region is an important contributor to increased wall stress both within the infarct and in the perfused regions of the heart and has been identified as a precipitating and sustaining phenomenon that drives adverse remodeling after MI. Infarct thickness was analyzed to evaluate the efficacy of the four treatment groups in preventing remodeling. Specifically, thicknesses in the apical infarct, basilar infarct, borderzone, and in the remote myocardium were measured for each treatment group, normal (non-infarcted) and for infarct control (IC) (Figure 4A, 4B). As expected, 8 weeks post-MI, IC animals displayed a significantly thinner myocardial wall in the apical and basilar infarct (apical: 2.2mm, basilar: 4.6mm) regions compared to normal non-infarct animals measured at areas corresponding to infarct regions in treatment animals (apical: 6.1mm, basilar: 8.5mm). MeHA treatment, as previously shown, was able to maintain thicknesses in the apical and basilar infarct at levels similar to normal tissue (low MeHA: apical: 6.5mm, basilar: 7.0mm, high MeHA: apical: 7.0mm, basilar: 7.2mm)<sup>18</sup>; this is due to the stability and minimal degradation behavior of these polymers. Interestingly, despite their hydrolytic degradation behavior, both HeMA-HA polymers increased the myocardium thickness compared to infarct controls, with significant increases observed in high HeMA-HA treatments in the apical infarct region but no significant increases in either polymer in the basilar infarct region (low HeMA-HA: apical: 3.5mm, basilar: 6.0mm, high HeMA-HA: apical: 4.1mm, basilar 6.1mm). HeMA-HA thickness increases, particularly low HeMA-HA increases, are not completely understood, but are thought to be due to a biological role of the material and degradation products (including neovascularization and inflammation), including HA as suggested by Yoon et al.<sup>25</sup>. Studies with fibrin, which is also degraded within 3 weeks, have shown similar results where despite degradation, fibrin was also effective in increasing myocardial thickness compared to IC<sup>15, 22</sup>.

Histological images of the tissue at 8 weeks provide insight into the amount of remaining gel at this time post-MI (Figure 5). As expected from the *in vitro* degradation assays, hydrogel was present in both MeHA formulations and to a minimal extent for the high HeMA-HA treatment group, primarily in the apex regions. There was no gel observed at this point for any of the low HeMA-HA groups in any of the locations. This observation supports the comparison of *in vitro* degradation analysis with these *in vivo* findings, as well as the limited enzymatic degradation that occurs to breakdown the stable HA hydrogels. Generally, there was extensive collagen staining in all of the groups, with more prominent staining for the low HeMA-HA formulations, potentially due to the released degradation products and changes in the inflammatory response.

Myocardial infarction results from the occlusion of an artery and leads to the depletion of oxygen and nutrients to the heart. To remedy this and salvage viable myocardium, groups have focused on restoring blood flow to ischemic tissue by stimulating vessel formation. While this has been successful via delivery of pro-angiogenic growth factors such as FGF<sup>51-54</sup>, VEGF<sup>55, 56</sup> and PDGF<sup>55</sup>, and molecules such as pleiotrophin<sup>57</sup>, other groups have also shown that biomaterials without angiogenic stimulants also hold the potential to

promote neovascularization<sup>58</sup>. In this investigation, immunohistochemical staining for  $\alpha$ -SMA was performed to assess the ability of our HA hydrogels to induce vessel formation.

Eight weeks post-MI, all four HA hydrogel groups resulted in an increase in vessel density in the BZ, middle, and apex regions of the heart compared to ICs (Figure 6), suggesting a role of HA hydrogel treatment in stimulating neovascularization. Significant improvements were seen when evaluating all vessels (Figure 6C) and thick vessels greater than 10 $\mu$ m (Figure 6E) between HeMA-HA hydrogel groups and ICs in the middle region of the infarct. In addition, both high mechanics hydrogel groups demonstrated significant increases in vessel density in the BZ region compared to ICs. No significant differences were observed when examining vessels with visible lumen (Figure 6D). In general, vessel quantification showed that HA treatment resulted in a similar degree of vessel formation in degradable and stable gels.  $\alpha$ -SMA positive staining in non-vessel forming cells was also observed, potentially indicative of myofibroblasts. While all treatment groups demonstrated more positive staining than IC, groups with hydrogel remaining 8 weeks post-MI (high HeMA-HA, low MeHA, and high MeHA), particularly stable MeHA hydrogels exhibited more pronounced staining around biomaterial implants (Figure 6A).

Inflammatory responses play a large role in tissue remodeling, which is important in the context of biomaterials for cardiac repair<sup>59, 60</sup>. To address this, an immunohistochemical evaluation with anti-MHC class II was performed to assess the degree of inflammation resulting from degradable and stable HA hydrogel treatments. MHC class II proteins are expressed on antigen presenting cells which include macrophages, dendritic cells and B lymphocytes; these cells present digested fragments of foreign extracellular antigens on their surface and are able to interact with helper T cells to stimulate an adaptive immune response<sup>61, 62</sup>. Examination of MHC Class II expressing cells, thus, provides a general idea of the inflammatory response of various hydrogels.

MHC Class II staining was analyzed in both the surrounding tissue and at the biomaterial interface, in groups where biomaterial was still present at 8 weeks. Staining in the surrounding tissue was generally limited to areas with vessels and as a result, all treatment groups displayed more positive MHC class II staining in this region (Figure 7). Although all groups exhibited more staining, both HeMA-HA groups, particularly high HeMA-HA, appeared to result in more prevalent staining in the surrounding tissue (Figure 7A). A similar observation was observed at the biomaterial interface, where high HeMA-HA resulted in more positive MHC class II staining around the hydrogel compared to stable degrading MeHA hydrogels (Figure 7B). According to *in vitro* work, high HeMA-HA hydrogels degrade within approximately 10 weeks; thus, it is expected that they are undergoing degradation and result in the release of fragments, which stimulate MHC class II expression, compared to stable gels which have limited degradation at 8 weeks.

The extent of LV dilation in treatment groups was compared to IC data by quantifying normalized end diastolic and systolic volumes (NEDV and NESV) from 3DE data after 2 and 8 weeks. As expected from previous studies,<sup>18</sup> both low polymers were not effective in preventing volume increases (Figure 8). Conversely, the high polymers revealed promising results at 2 weeks where both high polymers limited LV increases to a similar degree (high HeMA-HA: NEDV: 1.61 and NESV: 1.96, and high MeHA: NEDV: 1.62 and NESV: 1.89); however, at 8 weeks it was evident that the stable high MeHA was more effective (high HeMA-HA: NEDV: 1.98 and NESV: 2.46, and high MeHA: NEDV: 1.70 and NESV: 1.98). *In vitro* mechanical data supported these findings; while both high polymers had higher mechanics than myocardial tissue (~6 kPa) at 2 weeks<sup>18</sup>, high HeMA-HA mechanics were reduced to values lower than initial low values (~2 kPa) by 8 weeks. This finding supports the importance of the timing of mechanical support and suggests that myocardium



stabilization is required for a longer period of time (at least 8 weeks) to be most effective in attenuating LV dilation.

Functional improvements (CO and EF) were evaluated by comparing baseline to 2 and 8 weeks post-MI. No functional improvements were observed when comparing groups to baseline (Figure 9); all groups displayed worse CO and EF at 2 and 8 weeks, although, IC was the only group that demonstrated a statistically significant worse CO compared to the baseline (Figure 9A).

As already discussed, hydrogels were injected 30 minutes post-MI and evaluated at 2 and 8 weeks. Treatment was employed early to reduce the number of surgical interventions to prevent animal mortality. Other studies have injected materials as early as immediately after MI<sup>26</sup> and as late as two months<sup>19</sup>; most have shown improvement, with earlier injections before potential irreversible processes, resulting in more effective attenuation in LV remodeling<sup>19</sup>. Despite this, it is still not clear of the appropriate time for injection. The average time between MI symptom onset to hospital prevention is 2–6 hours<sup>65, 66</sup>, thus, a 30 minute injection time is not clinically feasible. Another implication to consider is the progression of the remodeling process; in this report, hydrogels were injected during the onset of necrosis and acute inflammation. The specific stage during which the hydrogel is injected, as well as the temporal properties from that injection point, may play a role in the overall outcomes.

## Conclusions

Hydrolytically degradable HA-based hydrogels were synthesized with tunable mechanics and degradation behavior and compared to stable HA hydrogels with similar mechanics and gel dispersion. When injected into early infarct tissue in an ovine model, these hydrogels demonstrated a similar vascular response to their stable gel counterpart; however, they also induced a stronger inflammatory response that may be associated with their degradation. Most interestingly, these hydrolytically degradable hydrogels revealed that geometrical and remodeling changes are dependent on the mechanical and degradation properties of the injected hydrogel. For example, wall thickness and NEDV and NESV were maintained better with a stable hydrogel, implying the temporal dependency of myocardial wall stabilization. While there was no functional improvement associated with either hydrolytic or stable hydrogels, all treatment groups displayed better CO than IC. These results illustrate the use of tunable hydrogel systems to probe the influence of particular material properties on adverse remodeling outcomes after infarction, specifically towards optimizing materials for this specific application.

## Acknowledgments

The authors would like to acknowledge the experimental assistance of Drs. Cindy Chung and Joshua Katz. This work was supported by a Wallace H. Coulter Early Career Investigator Award (JAB); National Institutes of Health grants HL63954 (RCG), HL73021 (JHG), HL76560 (JHG); and by individual Established Investigator Awards from the American Heart Association (JHG, RCG).

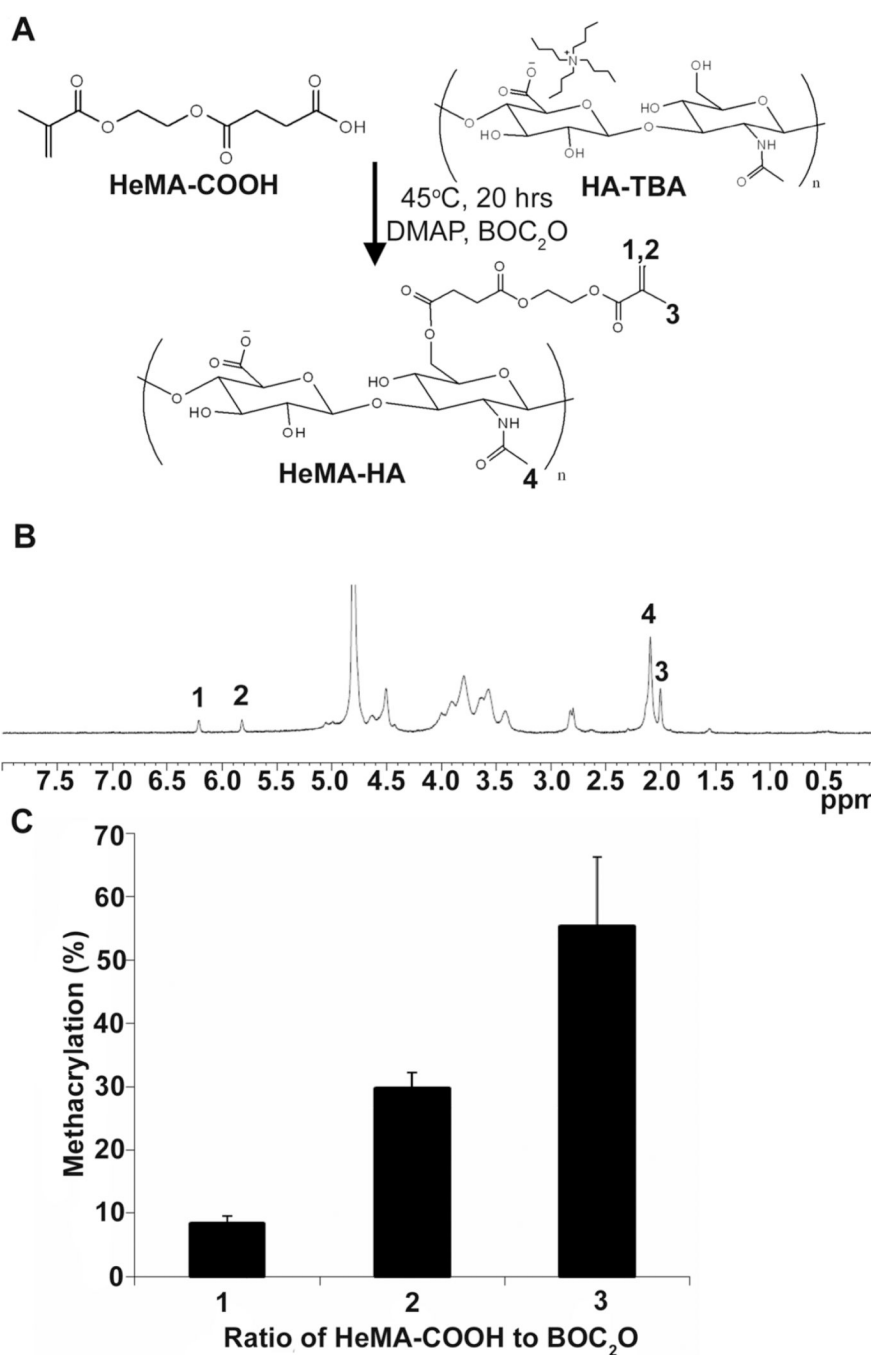
## References

1. Gheorghide M, Bonow RO. *Circulation*. 1998; 97(3):282–289. [PubMed: 9462531]
2. Holmes JW, Borg TK, Covell JW. *Annu Rev Biomed Eng*. 2005; 7:223–253. [PubMed: 16004571]
3. Pilla JJ, Gorman JH 3rd, Gorman RC. *Ann Thorac Surg*. 2009; 87(3):803–810. [PubMed: 19231393]
4. Kelley ST, Malekan R, Gorman JH 3rd, Jackson BM, Gorman RC, Suzuki Y, Plappert T, Bogen DK, Sutton MG, Edmunds LH Jr. *Circulation*. 1999; 99(1):135–142. [PubMed: 9884390]

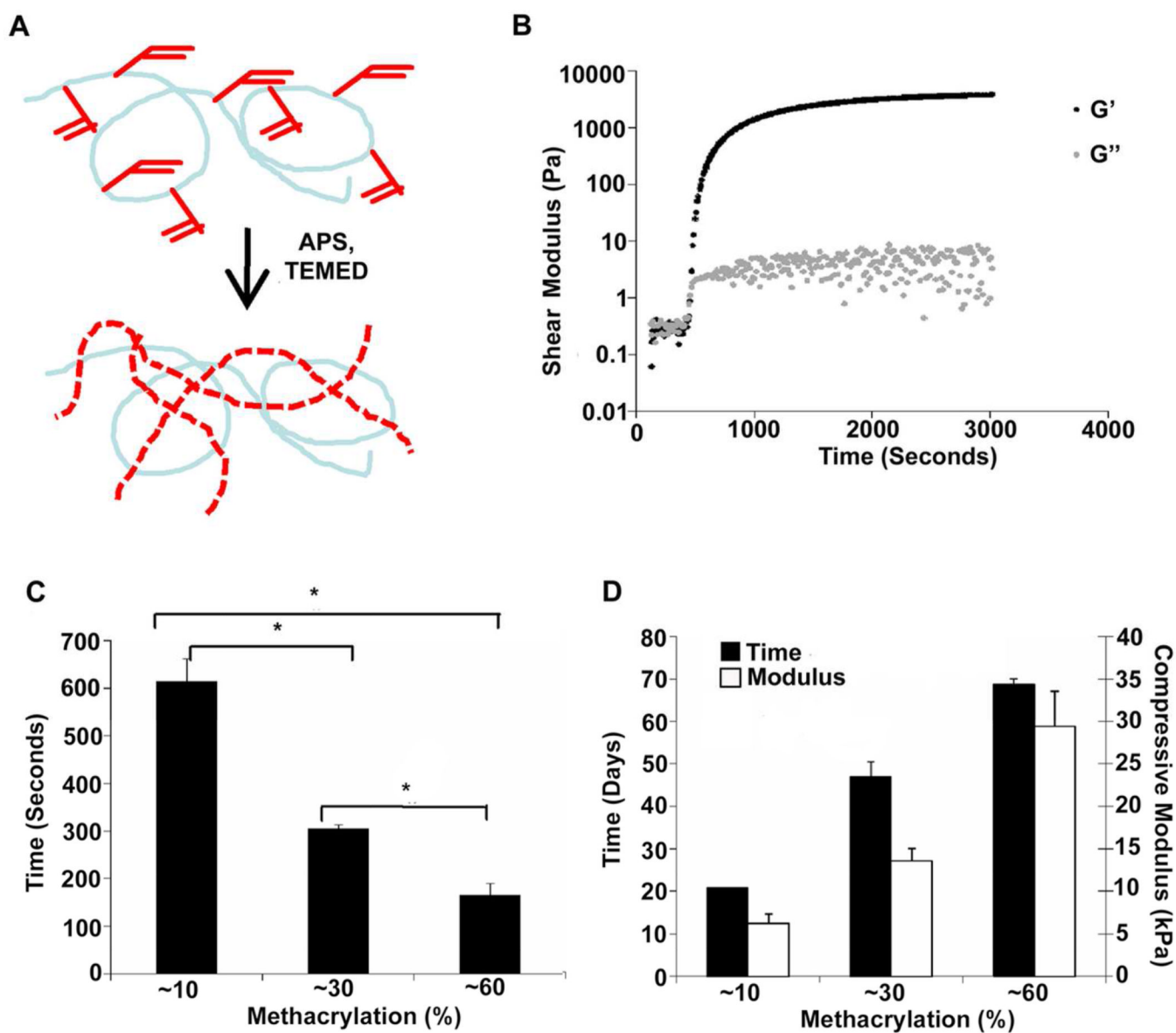
5. Jackson BM, Gorman JH 3rd, Salgo IS, Moainie SL, Plappert T, St John-Sutton M, Edmunds LH Jr, Gorman RC. *Am J Physiol Heart Circ Physiol*. 2003; 284(2):H475–H479. [PubMed: 12414441]
6. Epstein FH, Yang Z, Gilson WD, Berr SS, Kramer CM, French BA. *Magn Reson Med*. 2002; 48(2): 399–403. [PubMed: 12210951]
7. Frangogiannis NG, Smith CW, Entman ML. *Cardiovasc Res*. 2002; 53(1):31–47. [PubMed: 11744011]
8. Dobaczewski M, Gonzalez-Quesada C, Frangogiannis NG. *J Mol Cell Cardiol*. 48(3):504–511. [PubMed: 19631653]
9. Dang AB, Guccione JM, Mishell JM, Zhang P, Wallace AW, Gorman RC, Gorman JH 3rd, Ratcliffe MB. *Am J Physiol Heart Circ Physiol*. 2005; 288(4):H1844–H1850. [PubMed: 15604126]
10. Pfeffer MA, Braunwald E. *Circulation*. 1990; 81(4):1161–1172. [PubMed: 2138525]
11. Pfeffer MA, Pfeffer JM. *Circulation*. 1987; 75(5 Pt 2):IV93–IV97. [PubMed: 2952370]
12. Erlebacher JA, Weiss JL, Weisfeldt ML, Bulkley BH. *J Am Coll Cardiol*. 1984; 4(2):201–208. [PubMed: 6234343]
13. Wall ST, Walker JC, Healy KE, Ratcliffe MB, Guccione JM. *Circulation*. 2006; 114(24):2627–2635. [PubMed: 17130342]
14. Wenk JF, Wall ST, Peterson RC, Helgerson SL, Sabbah HN, Burger M, Stander N, Ratcliffe MB, Guccione JM. *J Biomech Eng*. 2009; 131(12):121011–121011-7.
15. Christman KL, Fok HH, Sievers RE, Fang Q, Lee RJ. *Tissue Eng*. 2004; 10(3–4):403–409. [PubMed: 15165457]
16. Christman KL, Vardanian AJ, Fang Q, Sievers RE, Fok HH, Lee RJ. *J Am Coll Cardiol*. 2004; 44(3):654–660. [PubMed: 15358036]
17. Dai W, Wold LE, Dow JS, Kloner RA. *J Am Coll Cardiol*. 2005; 46(4):714–719. [PubMed: 16098441]
18. Ifkovits JL, Tous E, Minakawa M, Morita M, Robb JD, Koomalsingh KJ, Gorman JH 3rd, Gorman RC, Burdick JA. *Proc Natl Acad Sci U S A*. 107(25):11507–11512. [PubMed: 20534527]
19. Landa N, Miller L, Feinberg MS, Holbova R, Shachar M, Freeman I, Cohen S, Leor J. *Circulation*. 2008; 117(11):1388–1396. [PubMed: 18316487]
20. Nelson DM, Ma Z, Fujimoto KL, Hashizume R, Wagner WR. *Acta Biomater*. 7(1):1–15. [PubMed: 20619368]
21. Tsur-Gang O, Ruvinov E, Landa N, Holbova R, Feinberg MS, Leor J, Cohen S. *Biomaterials*. 2009; 30(2):189–195. [PubMed: 18849071]
22. Yu J, Christman KL, Chin E, Sievers RE, Saeed M, Lee RJ. *J Thorac Cardiovasc Surg*. 2009; 137(1):180–187. [PubMed: 19154923]
23. Mukherjee R, Zavadzkas JA, Saunders SM, McLean JE, Jeffords LB, Beck C, Stroud RE, Leone AM, Koval CN, Rivers WT, Basu S, Sheehy A, Michal G, Spinale FG. *Ann Thorac Surg*. 2008; 86(4):1268–1276. [PubMed: 18805174]
24. Huang NF, Yu J, Sievers R, Li S, Lee RJ. *Tissue Eng*. 2005; 11(11–12):1860–1866. [PubMed: 16411832]
25. Yoon SJ, Fang YH, Lim CH, Kim BS, Son HS, Park Y, Sun K. *Journal of Biomedical Materials Research Part B: Applied Biomaterials*. 2008; 9:163–171.
26. Kofidis T, Lebl DR, Martinez EC, Hoyt G, Tanaka M, Robbins RC. *Circulation*. 2005; 112(9 Suppl) I173–I177.
27. Yu J, Gu Y, Du KT, Mihardja S, Sievers RE, Lee RJ. *Biomaterials*. 2009; 30(5):751–756. [PubMed: 19010528]
28. Leor J, Tuvia S, Guetta V, Manczur F, Castel D, Willenz U, Petnehazy O, Landa N, Feinberg MS, Konen E, Goitein O, Tsur-Gang O, Shaul M, Klapper L, Cohen S. *J Am Coll Cardiol*. 2009; 54(11):1014–10123.
29. Ryan LP, Matsuzaki K, Noma M, Jackson BM, Eperjesi TJ, Plappert TJ, St John-Sutton MG, Gorman JH 3rd, Gorman RC. *Ann Thorac Surg*. 2009; 87(1):148–155. [PubMed: 19101288]
30. Fujimoto KL, Ma Z, Nelson DM, Hashizume R, Guan J, Tobita K, Wagner WR. *Biomaterials*. 2009; 30(26):4357–4368. [PubMed: 19487021]

31. Jiang XJ, Wang T, Li XY, Wu DQ, Zheng ZB, Zhang JF, Chen JL, Peng B, Jiang H, Huang C, Zhang XZ. *J Biomed Mater Res A*. 2009; 90(2):472–477. [PubMed: 18546187]
32. Wang T, Jiang XJ, Lin T, Ren S, Li XY, Zhang XZ, Tang QZ. *Biomaterials*. 2009; 30(25):4161–4167. [PubMed: 19539990]
33. Wang T, Wu DQ, Jiang XJ, Zhang XZ, Li XY, Zhang JF, Zheng ZB, Zhuo R, Jiang H, Huang C. *Eur J Heart Fail*. 2009; 11(11):14–19. [PubMed: 19147452]
34. Toole BP. *Semin Cell Dev Biol*. 2001; 12(2):79–87. [PubMed: 11292373]
35. Burdick JA, Chung C, Jia X, Randolph MA, Langer R. *Biomacromolecules*. 2005; 6(1):386–391. [PubMed: 15638543]
36. Sahoo S, C C, Khetan S, Burdick J. *Biomacromolecules*. 2008; 8(4):5.
37. Khetan S, Burdick JA. *Biomaterials*. 31(32):8228–8234. [PubMed: 20674004]
38. Temenoff JS, Kasper FK, Mikos AG. *Topics in Tissue Engineering*. 2007; 3:1–16.
39. Platzer M, Ozegowski JH, Neubert RH. *J Pharm Biomed Anal*. 1999; 21(3):491–496. [PubMed: 10701415]
40. Ernst S, Langer R, Cooney CL, Sasisekharan R. *Crit Rev Biochem Mol Biol*. 1995; 30(5):387–444. [PubMed: 8575190]
41. Langer R, Peppas N. *J Macromol Sci-Rev Macromol Chem Phys*. 1983; C23(6):61–126.
42. Metters AT, Bowman CN, Anseth KS. *J Phys. Chem. B*. 2000; 104:7043–7049.
43. Metters AT, Anseth KS, Bowman CN. *Biomed Sci Instrum*. 1999; 35:33–38. [PubMed: 11143373]
44. Sawhney AS, Hubbell JA. *Biomaterials*. 1992; 13(12):863–870. [PubMed: 1457680]
45. von Burkersroda F, Schedl L, Gopferich A. *Biomaterials*. 2002; 23(21):4221–4231. [PubMed: 12194525]
46. Camenisch TD, Spicer AP, Brehm-Gibson T, Biesterfeldt J, Augustine ML, Calabro A Jr, Kubalak S, Klewer SE, McDonald JA. *J Clin Invest*. 2000; 106(3):349–360. [PubMed: 10930438]
47. Chen WY, Abatangelo G. *Wound Repair Regen*. 1999; 7(2):79–89. [PubMed: 10231509]
48. Laurent TC, Fraser JR. *FASEB J*. 1992; 6(7):2397–2404. [PubMed: 1563592]
49. Mataveli FD, Han SW, Nader HB, Mendes A, Kanishiro R, Tucci P, Lopes AC, Baptista-Silva JC, Marolla AP, de Carvalho LP, Denapoli PM, Pinhal MA. *Growth Factors*. 2009; 27(1):22–31. [PubMed: 19107652]
50. Rodgers LS, Lalani S, Hardy KM, Xiang X, Broka D, Antin PB, Camenisch TD. *Circ Res*. 2006; 99(6):583–589. [PubMed: 16931798]
51. Yamamoto T, Suto N, Okubo T, Mikuniya A, Hanada H, Yagihashi S, Fujita M, Okumura K. *Jpn Circ J*. 2001; 65(5):439–444. [PubMed: 11348050]
52. Iwakura A, Fujita M, Kataoka K, Tambara K, Sakakibara Y, Komeda M, Tabata Y. *Heart Vessels*. 2003; 18(2):93–99. [PubMed: 12756606]
53. Liu Y, Sun L, Huan Y, Zhao H, Deng J. *Eur J Cardiothorac Surg*. 2006; 30(1):103–107. [PubMed: 16730451]
54. Fujita M, Ishihara M, Morimoto Y, Simizu M, Saito Y, Yura H, Matsui T, Takase B, Hattori H, Kanatani Y, Kikuchi M, Maehara T. *J Surg Res*. 2005; 126(1):27–33. [PubMed: 15916971]
55. Hao X, Silva EA, Mansson-Broberg A, Grinnemo KH, Siddiqui AJ, Dellgren G, Wardell E, Brodin LA, Mooney DJ, Sylven C. *Cardiovasc Res*. 2007; 75(1):178–185. [PubMed: 17481597]
56. Wu J, Zeng F, Huang XP, Chung JC, Konecny F, Weisel RD, Li RK. *Biomaterials*. 32(2):579–586. [PubMed: 20932570]
57. Christman KL, Fang Q, Yee MS, Johnson KR, Sievers RE, Lee RJ. *Biomaterials*. 2005; 26(10):1139–1144. [PubMed: 15451633]
58. Tous E, Purcell B, Ifkovits JL, Burdick JA. *J Cardiovasc Transl Res*.
59. Anderson JM. *Annu. Rev. Mater. Res*. 2001; 31(20):81–110.
60. Anderson JM, Rodriguez A, Chang DT. *Semin Immunol*. 2008; 20(2):86–100. [PubMed: 18162407]
61. Alberts, B.; Johnson, A.; Lewis, J.; Raff, M.; Roberts, K.; Walter, P. *Molecular Biology of The Cell*. 4th Ed.. New York: Garland Science; 2002. p. 1392

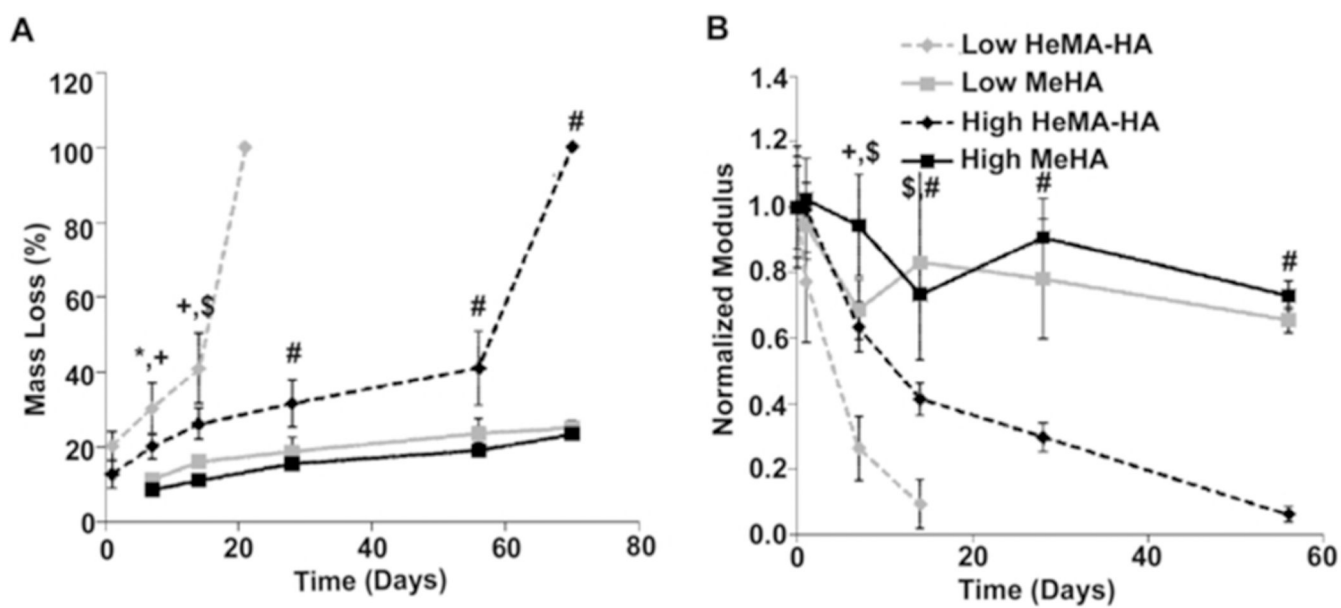
62. Mitchell, RN. *Biomaterials Science*. 2nd Ed. Ratner, BD.; Hoffman, AS.; Schoen, FJ.; Lemon, JE., editors. San Diego CA: Elsevier Academic Press; 2004. p. 304
63. Gage AA, Bhayana JN, Balu V, Hook N. *Arch Surg*. 1977; 112(12):1488–1492. [PubMed: 931636]
64. Lalka SG, Sawada SG, Dalsing MC, Cikrit DF, Sawchuk AP, Kovacs RL, Segar DS, Ryan T, Feigenbaum H. *J Vasc Surg*. 1992; 15(5):831–842. [PubMed: 1578539]
65. Jneid H, Fonarow GC, Cannon CP, Palacios IF, Kilic T, Moukarbel GV, Maree AO, LaBresh KA, Liang L, Newby LK, Fletcher G, Wexler L, Peterson E. *Circulation*. 2008; 117(19):2502–2509. [PubMed: 18427127]
66. Miura T, Miki T. *Basic Res Cardiol*. 2008; 103(6):501–513. [PubMed: 18716709]



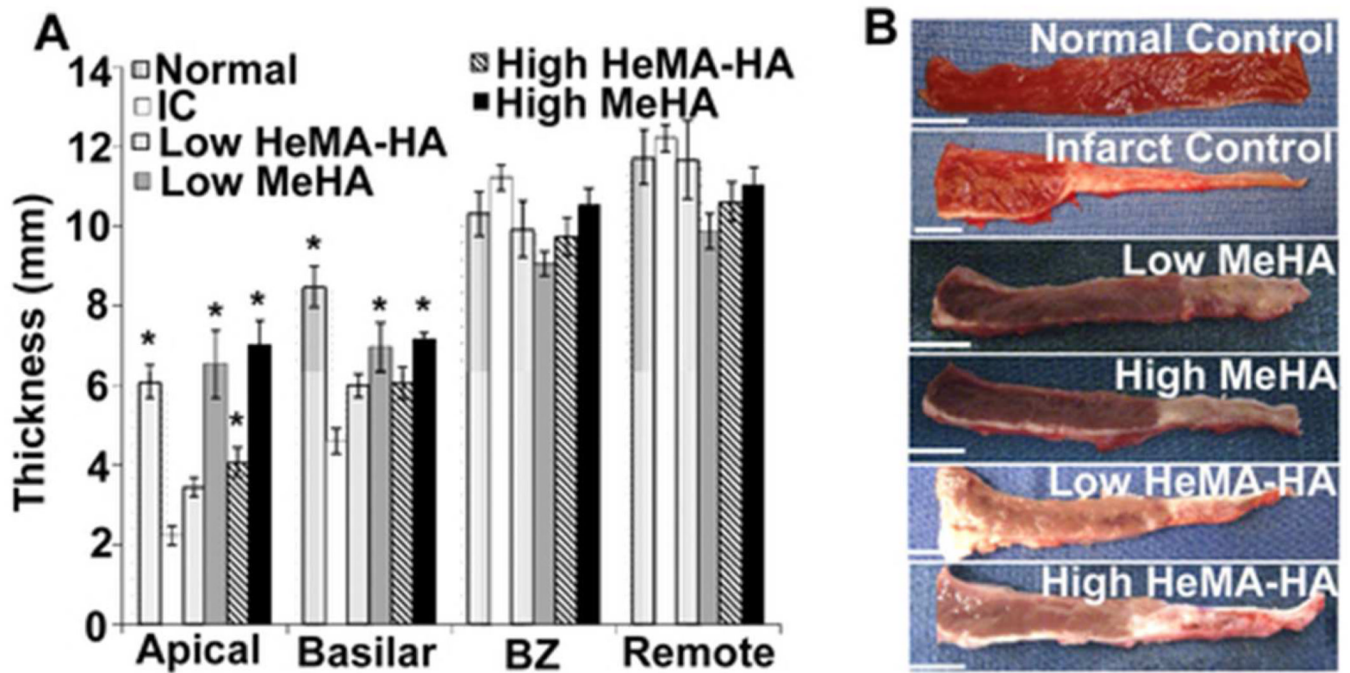
**Figure 1.** HeMA-HA synthesis and chemical structure (A) and representative <sup>1</sup>H NMR spectra where peaks 1 and 2 correspond to the protons on the alkene of the methacrylate, peak 3 is indicative of the methyl entity on the methacrylate, and peak 4 represents the protons on the N-acetyl group on the HA backbone; modification was determined by normalizing to peak 4 (B). The relationship between final methacrylation and HeMA-COOH to BOC<sub>2</sub>O ratio during synthesis, n=4 (C).



**Figure 2.** Schematic of hydrogel formation (A). Representative rheological time sweep after mixing HeMA-HA solutions containing either APS or TEMED, where the intersection of the storage and loss moduli is defined as the gel onset (B). Gel onset,  $n=3-4$ , (C) and degradation time and compressive modulus,  $n=3-4$ , (D) as a function of HeMA-HA methacrylation gelled at 5mM APS/TEMED. Data are presented as mean  $\pm$  SD. \* $p<0.05$ . All groups are statistically significant ( $p<0.05$ ) in panel D.



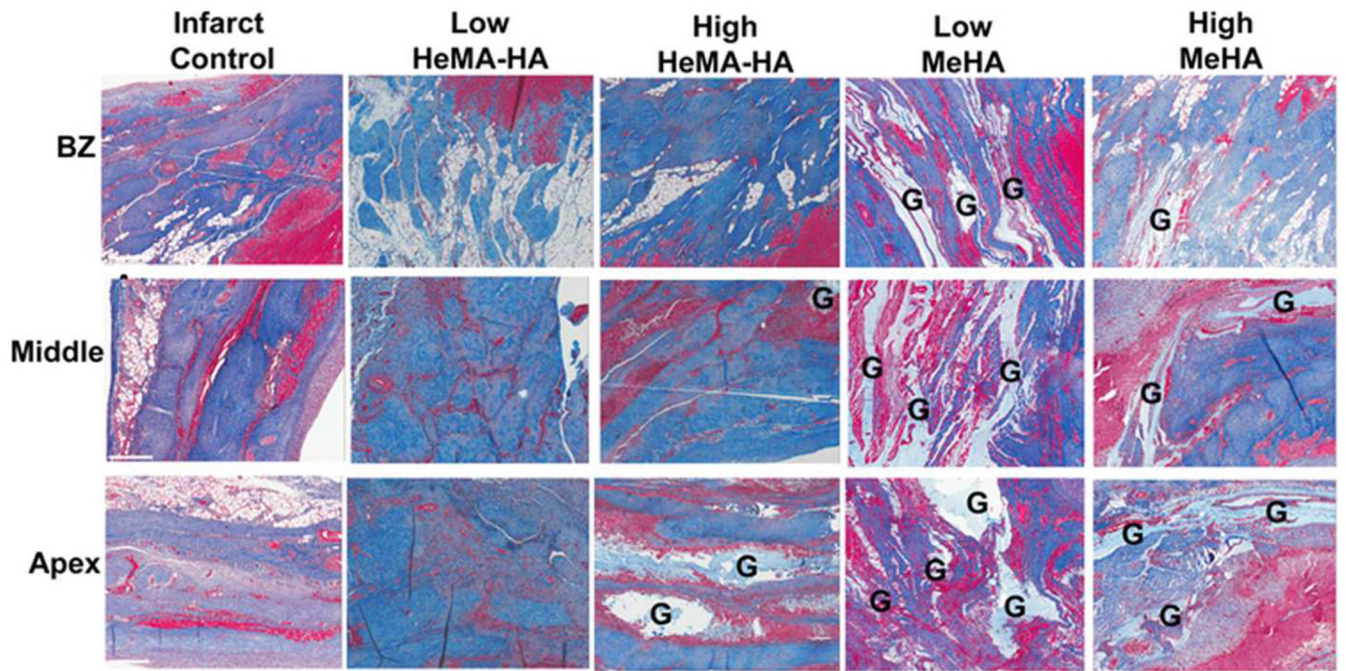
**Figure 3.** MeHA and HeMA-HA degradation,  $n=3-4$ , (A) and temporal mechanics profiles,  $n=3-4$  (B). \* $p<0.05$  Low HeMA-HA vs. Low MeHA, + $p<0.05$  High HeMA-HA vs. High MeHA, \$ $p<0.05$  Low HeMA-HA vs. all treatments, # $p<0.05$  High HeMA-HA vs. all treatments.



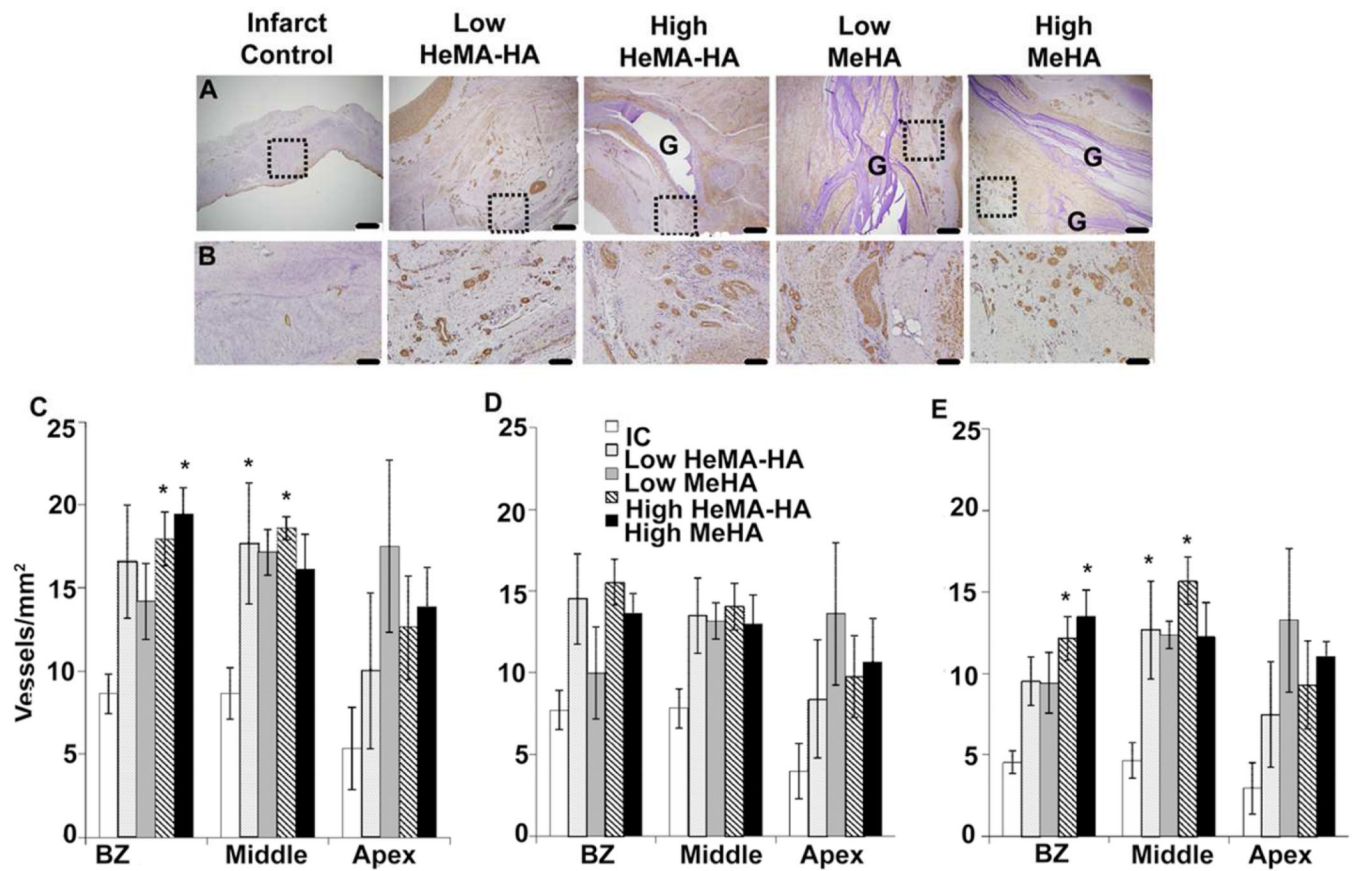
**Figure 4.**

*In vivo* evaluation of myocardium thickness of normal myocardium, infarct controls (IC), and HA treatment groups (A: quantified, B: images) 8 weeks post-MI. Data are presented as mean  $\pm$  SEM. \* $p < 0.05$  vs. IC. (Scale bar = 10 mm).



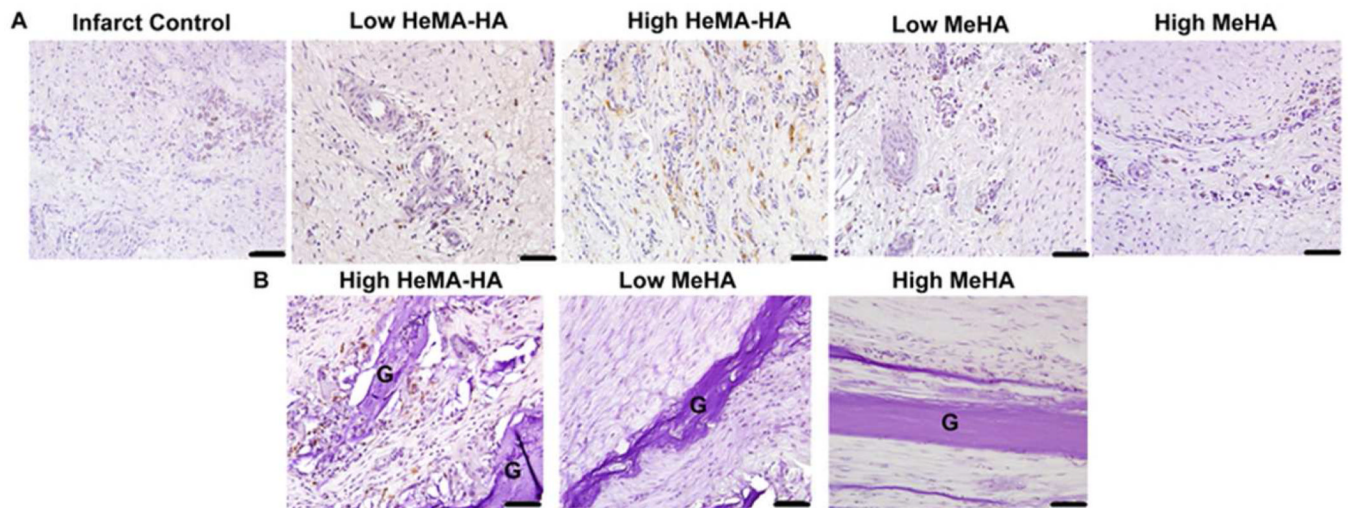


**Figure 5.** Histological evaluation (Masson's Trichrome stain) and representative images of treatment groups at borderzone (BZ), middle, and apex region infarct 8 weeks post MI. Scale bar= 500  $\mu\text{m}$ . G=Gel.

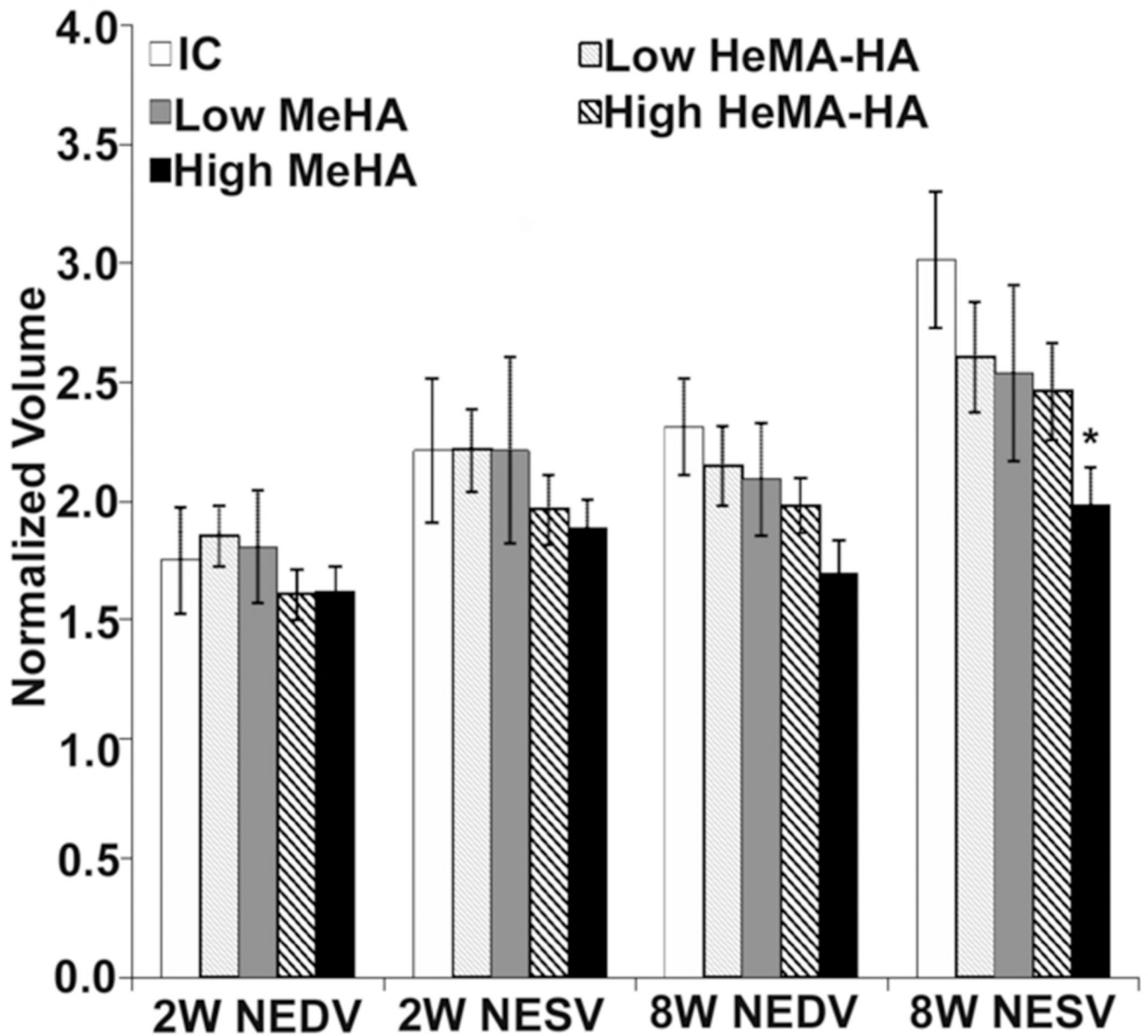


**Figure 6.**

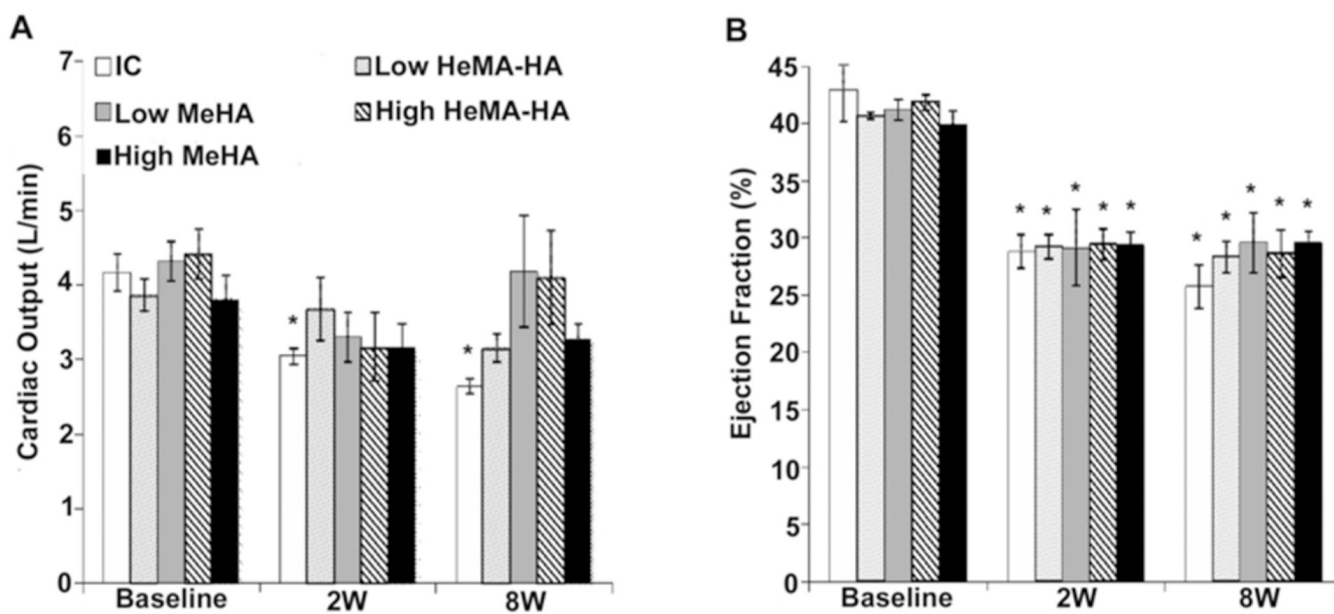
Immunohistochemical evaluation of  $\alpha$ -SMA for vessel formation. Representative images of myocardium cross section in middle region of infarct (Scale bar= 500  $\mu$ m) (A), and zoomed in representative images of vessels (Scale bar= 100 $\mu$ m) (B) in each group. Quantified vessel density of all vessels over 10 $\mu$ m (C), all vessels with lumen over 10 $\mu$ m (D), and all thick vessels over 10 $\mu$ m (E). Data are presented as mean  $\pm$  SEM. \* $p$ <0.05 vs. IC. G=Gel.



**Figure 7.** Immunohistochemical examination of inflammation with MHC Class II. Representative images in surrounding tissue in all groups (A) and representative images at biomaterial interface in all groups with biomaterial present at 8 weeks (B). (Scale bar= 50 $\mu$ m). G=Gel.


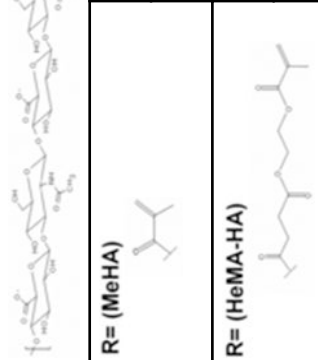


**Figure 8.** End diastolic and systolic volumes normalized to each treatment's respective baseline (NEDV and NESV) 8 weeks post MI. Data presented as mean  $\pm$  SEM. \* $p < 0.05$  vs. IC.



**Figure 9.** Cardiac output (CO) (A) and ejection fraction (EF) (B) of treatment groups at 2 and 8 weeks compared to their respective baseline values. Data are presented as mean  $\pm$  SEM. \* $p < 0.05$  vs. respective baseline.

Table 1

		Wt%	APS (A) and TEMED (T) Concentrations	Initial Mechanics	Degradation Time
 <b>R= (MeHA)</b>	Low	4	A: 5mM T: 5mM	7.73 ± 1.05 kPa	Stable
	High	4	A: 5mM T: 5mM	43.00 ± 12.40 kPa	Stable
 <b>R= (HeMA-HA)</b>	Low	4	A: 8mM T: 4mM	7.75 ± 2.44 kPa	~3 weeks
	High	4	A: 7mM T: 7mM	33.46 ± 0.84 kPa	~10 weeks